NONLINEAR DESIGN APPROACH OF A BROADBAND HYBRID INTEGRATED Ku-BAND COMMON-SOURCE GaAs FET VCO

R. Gratzl, J. Hausner, P. Russer

Institut f. Hochfrequenztechnik, Technische Universität München,
Arcisstr. 21, 8000 Munich 2, West Germany

Abstract

The design of a hybrid integrated Ku-Band voltage controlled oscillator is described. The oscillator was designed using linear theory based upon a linear FET-model extracted from measured transistor small signal S-parameters and then optimized for output power employing a nonlinear model for the internal FET. In the nonlinear model, the nonlinear transconductance and the nonlinear input admittance, caused by the Schottky-junction of the gate, were taken into account. The oscillator power was calculated by investigation of the amplitude of the fundamental wave caused by the dominating nonlinearities. Higher harmonics were not taken into account. With the optimized circuit and layout a tuning bandwidth from 12 GHz to 17.25 GHz with a corresponding output power of 7 dBm to 13.5 dBm was measured. Output power was within 2 dB of the predicted value over the whole tuning range.

Nonlinear Oscillator Modelling

To predict and optimize the oscillator output power, a nonlinear design approach is indispensable. The oscillator model depicted in Fig. 1 accounts for the dominating nonlinear effects of the active device. The oscillator circuit is subdivided into a linear feedback twoport and an active twoport[3]. The linear network contains the linear part of the FET-model which was derived from measured small signal S-parameters, and the linear oscillator circuit in which the FET was embedded. A description of the FET-model can be found in [1]. The linear oscillator circuit consists of the load matching network, the load, the microstrip-resonator, and the bias-networks. In the nonlinear twoport the dominating nonlinearities are represented by the transconductance and a nonlinear input admittance modelling the Schottky junction of the MESFET. The other nonlinear effects of the FET are neglected, e.g. the nonlinear capacitors are omitted to avoid the appearance of time derivatives in the nonlinear equations. This simplification is justified as other authors have also noted a dominant variation of S_{21} and consequently of the transconductance under large signal conditions [2].

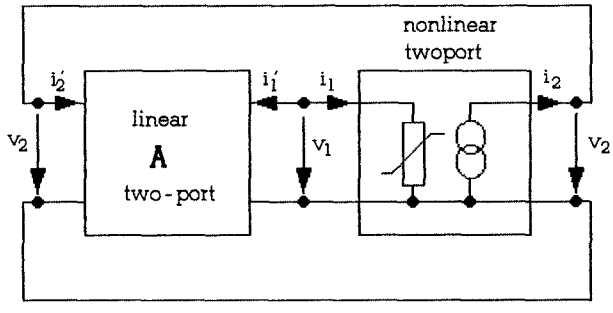

Figure 1: Separation of the oscillator circuit in a linear and a nonlinear subcircuit. The linear part of the FET-model is included in the linear subcircuit.

From the nonlinear relations in the time domain

$$i_1(t) = y(v_1(t)) \quad \text{and} \quad i_2(t) = s(v_1(t))$$

the amplitudes of the fundamental waves of the input and output currents $I_1(V_1)$ and $I_2(V_1)$, respectively are calculated. $y(v_1(t))$ describes the exponential chracteristic of the Schottky-junction whereas $s(v_1(t))$ represents the quadratic FET transfer characteristic, i.e. the nonlinear transconductance.

We assume a harmonic input voltage $v_1(t)$ with

$$v_1(t) = V_0 + V_1 \cdot \cos\psi \tag{1}$$

$$\psi = \omega_0 t + \phi \tag{2}$$

The expressions for the fundamental wave are

$$I_1(V_1) = \frac{1}{\pi}\int_0^{2\pi} y(v_1(t))\cos\psi d\psi \tag{3}$$

for the nonlinear gate admittance and

$$I_2(V_1) = \frac{1}{\pi}\int_0^{2\pi} s(v_1(t))\cos\psi d\psi \tag{4}$$

for the FET transfer characteristic.

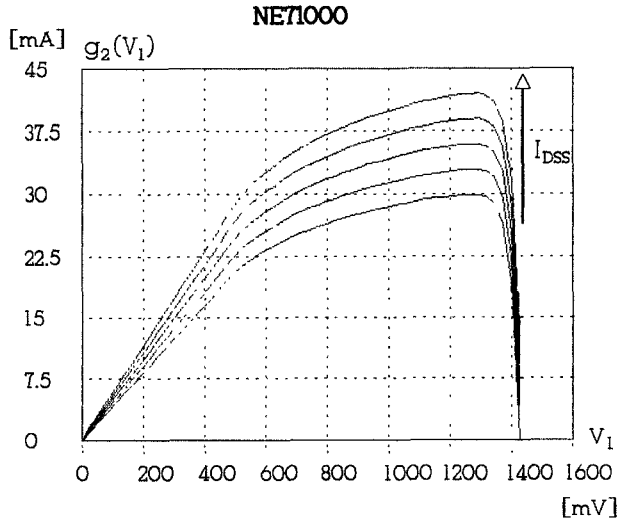

Figure 2: The fundamental wave amplitude of the output current $g_2(V_1)$ of the nonlinear twoport for several values of I_{DSS}

Together with the $\mathcal{ABCD}$-Matrix of the linear twoport **A** the following equation is obtained:

$$I_2(V_1) + \mathcal{D}I_1(V_1) + \mathcal{C}V_1 = 0 \tag{5}$$

Separating this into real- and imaginary parts for real V_1 and introducing the functions $g_1(V_1,\omega)$ and $g_2(V_1,\omega)$

$$g_1(V_1,\omega) = \mathrm{Im}\{\mathcal{D}(\omega)\}I_1(V_1) \tag{6}$$
$$g_2(V_1,\omega) = \mathrm{Re}\{\mathcal{D}(\omega)\}I_1(V_1) + I_2(V_1) \tag{7}$$

gives

$$g_1(V_1,\omega) + \mathrm{Im}\{\mathcal{C}\}V_1 = 0 \tag{8}$$
$$g_2(V_1,\omega) + \mathrm{Re}\{\mathcal{C}\}V_1 = 0 \tag{9}$$

Eq. (8) and Eq. (9) determine the frequency and the amplitude of the oscillation. Eq. (9) also contains the frequency dependence of the oscillation amplitude.

The function $g_2(V_1)$ is shown in Fig. 2 for various values of I_{DSS}. Due to Eq. (9) the curves are frequency dependent. However, this frequency dependence can be neglected in our case since $\mathrm{Re}\{\mathcal{D}\}$ does not vary much within the frequency range of interest. The resulting input amplitude V_1 and the corresponding output current $g_2(V_1)$ of the nonlinear current source is determined by the intersection of the feedback line $\mathrm{Re}\{\mathcal{C}\}V_1$ and $g_2(V_1)$ and thus the power delivered to the load can be calculated with a simple transformation described below.

Fig. 3 shows the feedback line for several frequencies (i.e. 12 GHz, 14 GHz, 17 GHz). The analysis of the linear circuit was performed using the SANA network analysis program[5].

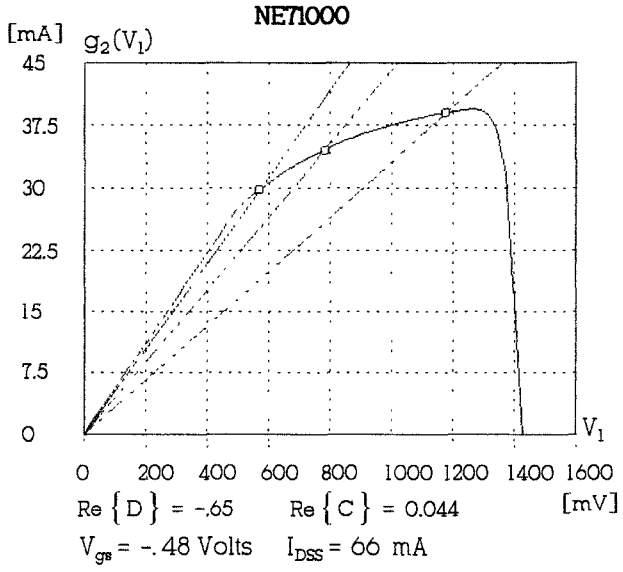

Figure 3: The intersection of the feedback line $\mathrm{Re}\{\mathcal{C}\}V_1$ and $g_2(V_1)$ for 12 GHz, 14 GHz and 17 GHz determines the amplitude of oscillation.

For a given amplitude of V_1 the equivalent resistance of the nonlinear Schottky-junction can be computed. This resistance is connected to port 1 of the linear twoport **A** and the circuit topology is rearranged to form a new twoport with the external port 1 at the output of the current source and the external port 2 at the load.

The equivalent circuit is depicted in Fig. 4. After calculation of the Z-Matrix of the rearranged linear twoport of Fig. 4 the current amplitude through the load can be obtained with the following equation:

$$I_L = I_2 \frac{-Z_{21}}{Z_{22} + Z_L} \tag{10}$$

From this we calculate the power delivered to the load.

Oscillator Circuit

The first design of the oscillator circuit was made by the linear theory[4]. Our examination of different circuit concepts has shown that a common source configuration with capacitive series feedback as shown in Fig. 5 has yielded the largest frequency tuning range. To ensure a potential unstable gate port of the transistor for frequencies up to 20 GHz a load matching network was designed utilizing stability circles. A quarter wave transformer provides the necessary low impedance load at the drain terminal of the transistor.

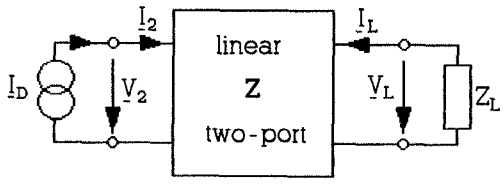

Figure 4: The rearranged twoport with the external load. The equivalent Schottky-junction impedance of the MESFET is included in the linear twoport **Z**.

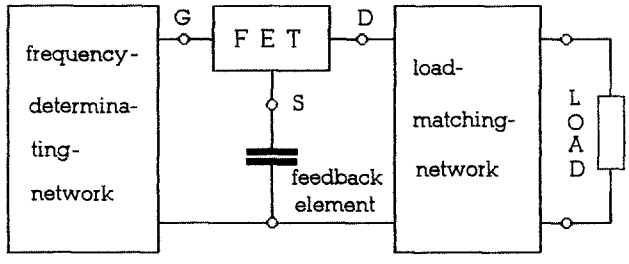

Figure 5: The basic oscillator topology in common source configuration. The feedback capacitor was realized utilizing a short microstrip open stub.

The frequency determining network consists of a microstrip resonator terminated by the hyperabrupt tuning varactor which together form a series resonant circuit. Fig. 7 shows the complete oscillator circuit. The FET, a NE71000, is biased by a source resistor consisting of ten thin film resistors alternating with small gold pads so that some resistors can be short circuited with gold bond wires. Therefore the bias point can be adjusted precisely, which is very useful since there are always some differences in the transistor pinch off voltages.

The gate is grounded by a high impedance thin film resistor connected to the microstrip resonator. This design does not degrade the rf-performance of the oscillator. The supply voltages of the drain and varactor are provided via rf-blocking networks consisting of radial stubs and microstrip rectangular inductors. CAD-programs SANA[5] as well as Touchstone [6] have been used successfully to model and optimize the linear subcircuit. The oscillator has been fabricated in hybrid integrated technology on a 10 mil alumina substrate in a size of 0.4 x 0.37 inches. Fig. 8 shows a photograph of the actual oscillator.

Results

With the knowledge of the behaviour of the nonlinear FET-twoport a power and bandwidth optimization can be done. Fig. 6 exhibits a plot of output power over frequency as

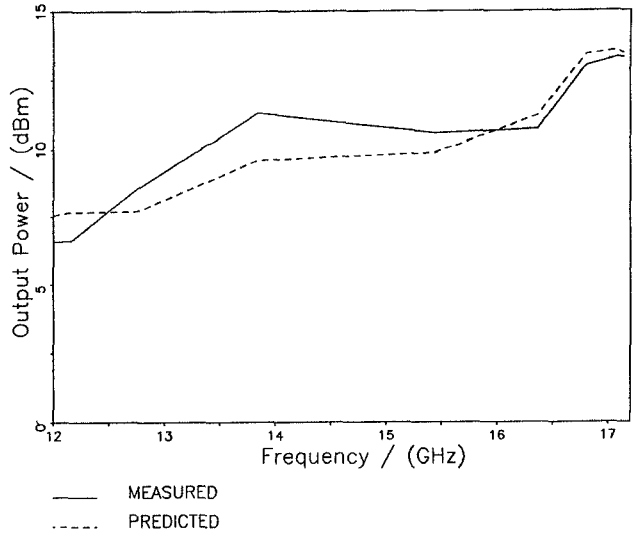

Figure 6: The predicted and measured output power versus frequency

obtained from measurement and calculation. The bandwidth and power were measured with an HP 8569A spectrum analyzer.

Power actually deviates less than 2 dB from the predicted value within the whole tuning range from 12.0 GHz up to 17.25 GHz. Using the hyperaprupt varactor CVG7864.70 from Alpha-Industries a linear tuning characteristic in a wide frequency range was obtained.

Conclusion

Using a simple nonlinear model of the FET requiring I_{DSS} as the only parameter, which can be easily measured, the output power of a broadband voltage controlled oscillator was predicted with good accuracy over the broad frequency range from 12.0 GHz to 17.25 GHz. Calculation of microwave oscillator output power need not be restricted to lenghty time domain computer simulation or rough estimates but can be quickly obtained by the method described above.

Acknowledgement

The authors would like to express their appreciation to Dr. Kaertner for his helpful discussions of this manuscript.

References

[1] A. Dupuis, J. Hausner, P. Russer: *Hybrid integrated Ku-band VCO*, Proc. of the 19th European Microwave Conference 1989, pp. 1009 – 1014

[2] C. Rauscher: Large-Signal Technique for Designing Single-Frequency and VC-GaAs-FET Oscillators. *IEEE Transactions on Microwave Theory and Techniques*, Vol. MTT-29, No. 4, April 1981, pp. 293 – 304

[3] P. Russer: *Informationstechnik Grundlagen*, VCH-Verlag, 1989 Weinheim, pp. 226 – 233

[4] G. Gonzales: *Microwave Transistor Amplifiers*, Prentice Hall, 1984, Englewood Cliffs, New Jersey

[5] Webb Laboratories: *SANA Manual*, 1989, Hartland, Wisconsin

[6] EEsof: *Touchstone Manual*, 1988, Westlake Village, California

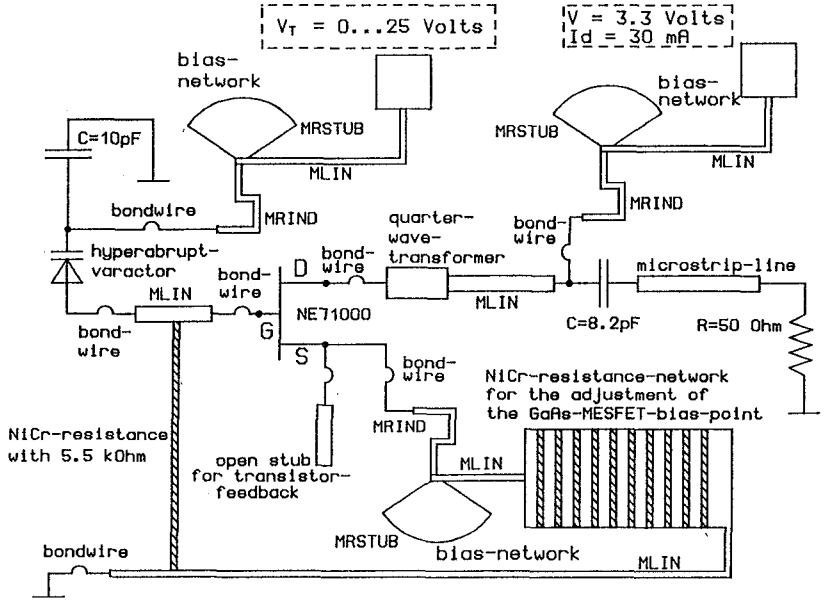

Figure 7: The complete oscillator circuit including the bias circuits for the transistor supply voltage as well as for the tuning voltage.

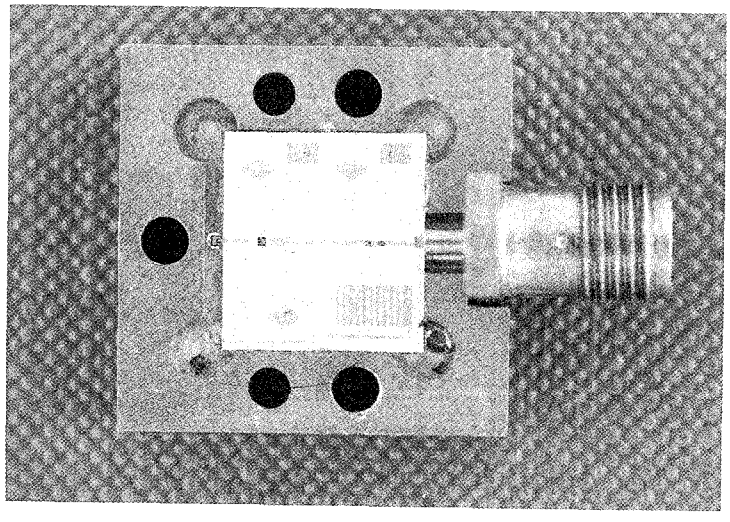

Figure 8: A photograph of the actual oscillator mounted in the bottom part of the microwave test fixture. The upper part of the fixture carrying the feed-through filters for the supply voltages is dismounted and not visible.